

# Quark structure and weak decays of heavy mesons

Stefan Resag and Michael Beyer

*Institut für Theoretische Kernphysik der Universität Bonn,  
Nussallee 14-16, 53115 Bonn, FRG  
FAX 0228-732328, Email:beyer@itkp.uni-bonn.de*

**Abstract:** We investigate the quark structure of  $D$  and  $B$  mesons in the framework of a constituent quark model. To this end, we assume a scalar confining and a one gluon exchange (OGE) potential. The parameters of the model are adopted to reproduce the meson mass spectrum. From a fit to ARGUS and CLEO data on  $B \rightarrow D^* \ell \nu$  semileptonic decay we find for the Cabibbo Kobayashi Maskawa matrix element  $V_{cb} = (0.036 \pm 0.003) (1.32ps/\tau_B)^{1/2}$ . We compare our form factors to the pole dominance hypothesis and the heavy quark limit. For non-leptonic decays we utilize factorization and for  $B \rightarrow D^{(*)} X$  decays we find  $a_1 = (0.96 \pm 0.05) (0.036/V_{cb})$ , and  $a_2 = (0.31 \pm 0.03)$ .

BONN TK-93-18

# 1 Introduction

Heavy mesons provide a rich and exciting tool to investigate the implications of fundamental interactions and symmetries. Numerous questions related to the dynamics of strong interaction, determination of standard model parameters, and the search for new physics have been addressed in this context.

Considerable amount of effort has been put into the description of mesons in terms of the underlying quark structure. For heavy mesons, viz. charmonium and bottomonium, non-relativistic models have been particularly successful in describing the mass spectra [1-11]. However, it has also been shown that relativistic effects may be quite significant in the transition observables of charmonium (and to some extent also in bottomonium), and generally, agreement with experimental data is improved [13]. For a review see e.g. [14, 15].

Here, we extend an earlier approach using a constituent quark model supplemented by relativistic corrections [13] to the case of unequal mass constituents. We address the questions of i) strong interaction dynamics to determine the mass spectrum, ii) relativistic effects in heavy-heavy and heavy-light quark systems, iii) form factors, and iv) semileptonic and non-leptonic decays.

The model is able to describe the meson mass spectrum for low radiative excitations to a satisfactory degree. However, for light mesons, it fails to reproduce the empirical decay observables. In particular for the  $\pi$  meson decay parameters such as the pion decay constant  $f_\pi$ , leptonic or  $\gamma\gamma$  decays cannot be described. This holds even with inclusion of relativistic corrections [16], because the  $\pi$  meson is treated as a rather strongly bound  $q\bar{q}$  system of constituent quarks of mass  $m_q \simeq m_N/3$ .

Some progress for the light mesons might be expected from recent developments using the Bethe-Salpeter equation for the  $q\bar{q}$  systems [17, 18, 19, 20]. However, technical and conceptional difficulties have restricted the use of the Bethe-Salpeter equation to approximate treatments, so far.

To circumvent some of the problems connected to light mesons that appear in non-leptonic decays, we follow the approach of Bauer, Stech and Wirbel (BSW) and introduce empirical values for the decay constants, if possible, to make our results less ambiguous [21].

In addition, for non-leptonic decays we utilize factorization. It has been proven quite useful, and seems to work reasonably well for  $B \rightarrow D^{(*)}X$  transitions [21], since final state interaction ( $fsi$ ) effects might be negligible in such cases. Also, it has been shown for  $D$  decays (at least for those that involve only one form factor) proper inclusion of  $fsi$  restores the validity of factorization to the level of experimental accuracy [23].

With the assumptions mentioned, we are now left with the determination of the two form factors for  $0^- \rightarrow 0^-$  transitions and the four form factors for  $0^- \rightarrow 1^-$  transitions. They will be calculated in the frame work of our model, which will briefly be surveyed in the next section. We compare our results to the

pole dominance ansatz to describe the  $q^2$  behavior of the form factors.

Recently, much attention has been paid to heavy quark effective theory (see e.g. [24] and references therein), which relates form factors of  $B \rightarrow D$  to those of  $B \rightarrow D^*$  transitions introducing heavy quark symmetries. All form factors are then related to one universal function (i.e. Isgur Wise function [25]). We will also compare our results to the idealized limit of heavy quarks.

Beside the description of the model, we also give the meson mass spectra in Sect. 2. In Sect. 3 we calculate form factors for semileptonic decays, which we also use in Sect. 4 where we give our results for non-leptonic decays. We summarize our main results and give our conclusion in Sect. 5.

## 2 The quark model

In the constituent quark model presented here, mesons are treated as quark-antiquark states, i.e. we do not consider any gluonic admixtures e.g.  $g\bar{q}q$ . Also no coupled channel effects are included although these might be relevant in some cases [2].

Confinement is modeled by a Lorentz scalar potential. As such it gives rise to a Darwin and a Thomas precession term in a  $(p/m)$  expansion. Furthermore, we assume that there is a residual short-range quark interaction from one-gluon-exchange which leads to spin and angular momentum dependent terms.

However, in agreement with earlier results in heavy quarkonia, we found that not all terms are equally important. Differences between a full version and a reduced version are rather small on the average (see also discussion in [13]). For the low lying states of  $c\bar{s}$ ,  $b\bar{s}$ ,  $c\bar{b}$ , this conclusion is in qualitative agreement with the findings of Lichtenberg, Roncaglia and Wills who investigated the influence of different potential models in these systems [11]. In addition due to the mesons considered here, viz.  $0^-$  and  $1^-$  mesons only, not all ingredients of the Hamiltonian contribute due to selection rules. In particular spin-orbit interactions do not contribute in the model space chosen here. We define

$$H = M + T + V_C + V_R + W_R^T + W_R^{SS} \quad (1)$$

where  $M$  is the sum of the constituent quark masses  $m_q$ ,  $m_{\bar{q}}$ , and  $T$  the kinetic energy of relative motion in the center of mass system,

$$V_C = a + br \quad (2)$$

$$V_R = -\frac{4}{3} \frac{\alpha_s}{r} \quad (3)$$

and the spin dependent forces

$$(4)$$

$$W_R^T = \frac{1}{3m_q m_{\bar{q}}} S_{q\bar{q}} \left( \frac{1}{r} V_R^{C'}(r) - V_R^{C''}(r) \right) \quad (5)$$

$$W_R^{SS} = \frac{2}{3m_q m_{\bar{q}}} (\mathbf{s}_q \cdot \mathbf{s}_{\bar{q}}) (\Delta V_R^C)(r) \quad (6)$$

In the above expressions,  $\mathbf{r}$  denotes the relative distance between quark and antiquark,  $\mathbf{s}_q$  and  $\mathbf{s}_{\bar{q}}$  are the respective spins,  $\mathbf{S} = \mathbf{s}_q + \mathbf{s}_{\bar{q}}$  the total spin operator, and  $S_{q\bar{q}} = 3\mathbf{s}_q \cdot \hat{\mathbf{r}}\mathbf{s}_{\bar{q}} \cdot \hat{\mathbf{r}} - \mathbf{s}_q \cdot \mathbf{s}_{\bar{q}}$  the tensor operator ( $\hat{\mathbf{r}} = \mathbf{r}/r$ ). The quark masses and the parameters of the potentials, the off-set  $a$ , the string tension  $b$ , and the coupling strength  $\alpha_s$  are treated as free parameters. They are adjusted to reproduce the experimental meson spectra shown in Fig. 1. Parameter values are shown in Table 1.

We note here, that since we do not use a perturbative treatment of the residual interaction, we need to regularize the potentials in order to prevent presumably spurious [26] divergences, see also [13]. We choose

$$1/r \rightarrow \sum_{i=1}^5 \beta_i \exp[-\gamma_i^2 r^2] \quad (7)$$

for the residual interaction, and

$$b \rightarrow b(r) = b \cdot (1 - \exp[-(r/2r_0)^2]) \quad (8)$$

for the confining interaction. The parameters  $\beta_i$ ,  $\gamma_i$  are fixed to fit  $1/r$  with maximum likelihood in the region between  $r_0$  and  $4r_0$ , where  $r_0$  is given in Table 1.

The regularized Hamiltonian is then diagonalized in a reasonably large basis. We have used a Laguerre (in momentum space) as well as an oscillator basis, and found only marginal differences in the spectra. In fact, results presented are calculated using the Laguerre basis, with the advantages that the number of necessary basis states is smaller and that the treatment of higher relative momenta is more realistic due to the asymptotic behaviour of the Laguerre polynomials. This might be of particular importance for small values of four momentum transfers  $q^2$ , viz. large three momentum  $\mathbf{q}^2$  in the rest frame of the decaying particle.

The energy eigenvalues are then obtained by minimizing the expectation value with respect to the basis parameter due to Ritz' variational principle. The minima occurring are rather flat, thus independent of the specific choice of the variational parameter. Therefore it is possible to choose the same parameter for all mesons.

The spectra for  $0^-$  and  $1^-$  mesons are shown in Fig. 1. We have excluded all other mesons from the figure, since they are not relevant for the present purpose. However, they have been included in the fitting procedure that lead to the parameter values given in Table 1. To this end all pieces of the Hamiltonian, such as e.g. the spin-orbit interaction (but no additional parameters), have been retained [27]. The overall agreement of the model with the experimental values is quite satisfactory.

The masses found for the constituent quarks are in agreement with the values found by [11] for five different potential models. Also our value for the off-set  $a$  is close to the respective values of Cornell [2], Song-Lin [10], Turin [11], and Indiana [7] potential, also studied by [12]. The value for  $b$  is slightly smaller and  $\alpha_s$  slightly larger than the respective values of the Cornell potential, which has the same  $r$ -dependence of  $V_C$  and  $V_R$ . Part of the differences may be attributed to differences in the spin dependent part of the interaction, but we do not go into further details here.

The different values of  $r_0$  introduced to regularize the potential due to different constituent quark masses  $m_q$  quoted in Table 1, are not surprising and can be understood qualitatively. It may be interpreted as an effective extention of the constituent quark (which in fact may be a complicated object) or through the “smearing” of the potential due to relativistic effects [28].

### 3 Form factors and semileptonic decays

Semileptonic decays are treated in current-current approximation. Since we are mainly concerned about  $b \rightarrow c$  transitions we give all formulas for that case only. Generalisation to different flavor dependence is straight forward. The Lagrangian is then given by

$$\mathcal{L}_{cb} = \frac{G_F}{\sqrt{2}} V_{cb} h_{cb}^\mu j_\mu \quad (9)$$

with the Cabibbo-Kobayashi-Maskawa matrix element  $V_{cb}$ . The leptonic  $j_\mu$  and hadronic currents  $h_{cb}^\mu$  are defined by

$$j_\mu = \bar{\ell} \gamma_\mu (1 - \gamma_5) \nu_\ell \quad (10)$$

$$h_{cb}^\mu = \bar{c} \gamma^\mu (1 - \gamma_5) b \quad (11)$$

The relevant transition amplitudes for  $B \rightarrow D$  and  $B \rightarrow D^*$  of the hadronic current can be decomposed due to the Lorentz covariance of the current, thus introducing form factors. For  $0^- \rightarrow 0^-$  transitions we use

$$\begin{aligned} \langle D, P_D | h_{cb}^\mu | B, P_B \rangle = \\ \left( P_B + P_D - \frac{m_B^2 - m_D^2}{q^2} q \right)^\mu F_1(q^2) + \frac{m_B^2 - m_D^2}{q^2} q^\mu F_0(q^2) \end{aligned} \quad (12)$$

with  $q^\mu = (P_B - P_D)^\mu$ , and  $F_0(0) = F_1(0)$ . In the case of  $0^- \rightarrow 1^-$ , the appropriate current may be parametrized as follows

$$\begin{aligned} \langle D^*, P_{D^*} \varepsilon | h_{cb}^\mu | B, P_B \rangle = \\ \frac{2}{m_B + m_{D^*}} \epsilon_{\nu\rho\sigma}^\mu \varepsilon^{*\nu} P_B^\rho P_{D^*}^\sigma V(q^2) - i \varepsilon^* \cdot q \frac{2m_{D^*}}{q^2} q^\mu A_0(q^2) \end{aligned}$$

$$\begin{aligned}
& - i(m_B + m_{D^*}) \left( \varepsilon^* - \frac{\varepsilon^* \cdot q}{q^2} q \right)^\mu A_1(q^2) \\
& + \frac{i\varepsilon^* \cdot q}{m_B + m_{D^*}} \left( P_B + P_{D^*} - \frac{m_B^2 - m_{D^*}^2}{q^2} q \right)^\mu A_2(q^2)
\end{aligned} \tag{13}$$

with  $\varepsilon^\nu$  polarization vector of  $D^*$ ,  $\epsilon_{\mu\nu\rho\sigma}$  antisymmetric tensor, and the restriction

$$2m_{D^*}A_0(0) = (m_B + m_{D^*}) A_1(0) - (m_B - m_{D^*}) A_2(0) \tag{14}$$

Note that  $0 < q^2 < q_{max}^2 = (m_B - m_{D^{(*)}})^2$  due to kinematical reasons. With the parametrization given above, it is straight forward to evaluate observables. They have been given by Körner and Schuler in a series of papers and formulas which will not be repeated here [32].

Our concern is to determine the form factors. For special values, e.g. at  $q^2 = 0$  or  $q^2 = q_{max}^2$ , the form factors may be fixed due to (approximate) flavour symmetries and a conserved vector current.

It has been argued that at  $q^2 \simeq q_{max}^2$ , i.e. small three momentum transfer, values of the form factors may be fixed with a nonrelativistic model. This has been utilized by Godfrey and Isgur, who use  $m_q + m_{\bar{q}}$  instead of experimental meson masses  $\mu$  and connect their arguments to the Lorentz representation of free particles [28].

A different possibility is to assume pole dominance. Such poles may occur, if strong interaction processes dominate the decay dynamics, and poles are formed prior to decay. This has been widely used by Bauer, Stech and Wirbel (BSW) [21], and also Körner and Schuler (KS) [32] but with different pole types and different values at  $q^2 = 0$ . BSW use ad hoc wave functions of the relativistic harmonic oscillator (in the infinite momentum frame) to fix the value at  $q^2 = 0$ . KS assume all ( $B \rightarrow D^{(*)}$ ) form factors normalized to 0.7 at  $q^2 = 0$ . Both models are compared to our results in the following, see Fig. 2.

In order to evaluate the current matrix elements (i.e. l.h.s. of (12) and (13)) from a quark model to determine the form factors, we introduce a Fock-space representation for mesons. This has been done e.g. by van Royen and Weisskopf [30] and by Godfrey and Isgur [28]. We follow their suggestion with minor changes. This procedure allows us to introduce relativistic corrections in the current operators as will be explained now.

The meson is represented as a superposition of free quark states, and the amplitudes are given in terms of the meson wave function in momentum space, viz.

$$\begin{aligned}
|\omega, \mathbf{P}\rangle &= \sqrt{2\omega} \int \frac{d^3 p}{(2\pi)^3} \frac{1}{\sqrt{2p_q^0 2p_{\bar{q}}^0}} \\
&\times \sum_{LS} R_{NLS}(p) [Y_L(\hat{\mathbf{p}}) \otimes \chi_S]^{[J]} \chi_F \chi_C \left| \frac{m_q}{M} \mathbf{P} + \mathbf{p} \right\rangle_q \left| \frac{m_{\bar{q}}}{M} \mathbf{P} - \mathbf{p} \right\rangle_{\bar{q}}
\end{aligned} \tag{15}$$

where  $\mathbf{p}_q$ ,  $\mathbf{p}_{\bar{q}}$  are the quark momenta,  $p_q^0 = \sqrt{\mathbf{p}_q^2 + m_q^2}$  (and analogously for  $\bar{q}$ ). The total momentum is given by  $\mathbf{P} = \mathbf{p}_q + \mathbf{p}_{\bar{q}}$ , and the relative momentum by  $M\mathbf{p} = m_{\bar{q}}\mathbf{p}_q - m_q\mathbf{p}_{\bar{q}}$ . The quarks are normalized with  $\langle \mathbf{p}'_q | \mathbf{p}_q \rangle = (2\pi)^3 2p_q^0 \delta(\mathbf{p}'_q - \mathbf{p}_q)$ . The spin, flavor, and color wave functions are denoted by  $\chi_S$ ,  $\chi_F$ ,  $\chi_C$ , respectively. The momentum space wave function is given by  $R_{NLS}(p)Y_L(\hat{\mathbf{p}})$ . Using the experimental meson mass  $\mu$ , the free energy of the meson is  $\omega = \sqrt{\mathbf{P}^2 + \mu^2}$ . Thus the normalization chosen in (15) differs from [28], and is given by  $\langle \mathbf{P}' | \mathbf{P} \rangle = (2\pi)^3 2\omega \delta(\mathbf{P}' - \mathbf{P})$ .

The current operator (11), evaluated between the meson wave function given in (15) lead to the following single quark matrix elements,

$$\langle p'_q | h_{cb}^\mu | p_q \rangle = (2\pi)^4 \delta^{(4)}(p_q - p'_q - q) \bar{u}_{q'}(p'_q) \gamma^\mu (1 - \gamma_5) u_q(p_q) \quad (16)$$

This way it is possible to take into account (relativistic) effects induced through the full Dirac quark spinor. In the following the nonrelativistic result quoted is achieved by taking the lowest order  $p/m$  in the above matrix element, and neglecting the momentum dependence in the normalization of (15).

We then evaluate the hadronic matrix elements using (15) in the laboratory system. Although this approach is not a covariant formalism, it is a natural way to include relativistic effects into the calculation of decays in a nonrelativistic quark model. For heavy mesons this formalism should be appropriate since  $p/m$  is small in these mesons.

In Fig. 2 we give the form factors relevant for the transition of  $B \rightarrow D$  and  $B \rightarrow D^*$ . They are calculated using the wave functions consistent with the Hamiltonian (1), and reproducing the mass spectra as shown in Fig. 1. Our calculation is given by the solid line. The (mono) pole dominance ansatz of BSW is shown as a dashed line. The parameters of BSW are given in Table 2. Schuler and Körner use a single pole mass of  $m_{pole} = 6.34\text{GeV}$ . The form factors  $F_1$  and  $A_1$  are assumed monopole, but opposite to BSW,  $A_2$  and  $V$  are assumed dipole behaviour and shown as dotted line [32]. Our results differ strongly to the (di-) pole ansatz.

In general our result is larger than the BSW model, so that a smaller  $V_{cb}$  can be expected than has been found by [21]. Taking only nonrelativistic terms as explained above we find even larger form factors than the full calculation. They differ less at  $q^2 = q_{max}^2$  (as expected) but rather strongly at  $q^2 = 0$ . The form factor  $A_2$  is only slightly changed. The nonrelativistic results are shown as dashed-dotted curves in Fig. 2.

Since the model is not covariant, form factors usually depend on the reference frame. As a test, we evaluated  $0^- \rightarrow 0^-$  transitions in the  $D$  rest frame also. Differences in the from factors are generally smaller than 10%. At  $q^2 = 0$  we found differences of a few per cent only compared to the calculation in the  $B$  rest frame .

The exclusive decay spectrum is shown in Fig. 3. We compare our results to recent ARGUS [31] and CLEO data [33, 34]. We find a best fit with  $V_{cb} = (0.036 \pm 0.003)(1.32ps/\tau_B)^{1/2}$ . The error resulting from  $\chi^2$  fitting is indicated by the upper and lower dotted line.

The resulting total branching ratios for semileptonic  $B$  decays agree well with experimental data given by the Particle Data Group [35] or more recently by the CLEO collaboration [34] and ARGUS collaboration [31]. They are given in Table 3.

In Figs. 4 and 5 we give the resulting forward backward asymmetry  $A_{FB}$  and the asymmetry parameter  $\alpha$  defined e.g. in [32] as a function of the lepton cut-off momentum. The forward backward asymmetry sensitive to parity violation is defined through

$$A_{FB} = \frac{N_F - N_B}{N_F + N_B} \quad (17)$$

with  $N$  the number of leptons in forward, resp. backward hemisphere in the rest system of the  $W$ -boson. For  $A_{FB}$  we have used a symmetric cut on the lepton momentum  $p_\ell$  as utilized by the CLEO collaboration [34] for technical reasons.

The helicity alignment  $\alpha$  describes the  $D^{*+}$  polarization extracted from the  $D^{*+} \rightarrow D^0\pi^+$  decay angle distribution  $W(\theta^*)$ , viz.

$$W(\theta^*) \propto 1 + \alpha \cos^2 \theta^* \quad (18)$$

For  $\alpha$  only a lower cut has been introduced. Both observables are in good agreement with experimental results. For comparison we have included the results of Körner-Schuler given in [32] as a dotted curve.

We would now like to connect our results to the notion of heavy quark symmetry. In this context form factors  $h_\pm(\omega)$ , and  $h_V(\omega)$ ,  $h_{A_{1,2,3}}(\omega)$  are introduced. They are related to the ones introduced above for  $0^- \rightarrow 0^-$  via

$$h(\omega)_\pm = \frac{m_B \pm m_D}{2\sqrt{m_B m_D}} F_1(q^2) + \frac{m_B \mp m_D}{2\sqrt{m_B m_D}} \frac{m_B^2 - m_D^2}{q^2} (F_0(q^2) - F_1(q^2)) \quad (19)$$

and for  $0^- \rightarrow 1^-$  via

$$h(\omega)_V = \frac{2\sqrt{m_B m_{D^*}}}{m_B + m_{D^*}} V(q^2) \quad (20)$$

$$h(\omega)_{A_1} = \frac{m_B + m_{D^*}}{(\omega + 1)\sqrt{m_B m_{D^*}}} A_1(q^2) \quad (21)$$

$$h(\omega)_{A_2} = \sqrt{\frac{m_B}{m_{D^*}}} (A_+(q^2) - A_0(q^2)) \quad (22)$$

$$h(\omega)_{A_3} = \sqrt{\frac{m_{D^*}}{m_B}} (A_-(q^2) + A_0(q^2)) \quad (23)$$

where we have introduced  $A_{\pm}(q^2)$  for convinience.

$$A_{\pm}(q^2) = \left( \frac{m_B}{m_B + m_{D^*}} \pm \frac{m_B(m_B + m_{D^*})}{q^2} \right) A_1(q^2) \mp \frac{m_B(m_B - m_{D^*})}{q^2} A_2(q^2) \quad (24)$$

In case of ideal heavy quark limit,

$$h_V(\omega) = h_{A_1}(\omega) = h_{A_3}(\omega) = h_+(\omega) = \xi(\omega) \quad (25)$$

$$h_{A_2}(\omega) = h_-(\omega) = 0 \quad (26)$$

with

$$\omega = \frac{m_B^2 + m_{D^{(*)}}^2 - q^2}{2m_B m_{D^{(*)}}} \quad (27)$$

Note, that we have not employed the limit  $m_{D^{(*)}}, m_B \rightarrow \infty$ . The wave functions reproduce the meson mass spectrum and therefore the overlap at  $q^2 = q_{max}^2$ , viz.  $\omega = 1$ , cannot be expected to be complete. Nevertheless, the ideal limit of  $\xi(1) = 1$  is realized within a few per cent, see Table 4. We find it possible to fit the  $\omega$  dependence of the dominant form factor by a simple function, viz.

$$h(\omega) = h(1) \cdot (1 + \beta(1 - \omega)) \quad (28)$$

with the parameters given in Table 4. The deviations from the fit are smaller than 1%, viz. smaller than the model uncertainties expected.

The form factor  $h_-(\omega)$  is small as expected from heavy quark limit. The form factor  $h_{A_2}(\omega)$  has been multiplied by  $r = m_{D^*}/m_B \simeq 0.38$  since this is the relevant quantity entering in the helicity amplitudes. This way the magnitude of the form factor  $rh_{A_2}(\omega)$  can directly be compared to  $h_{A_3}(\omega)$ .

It seems that the heavy quark limit is fulfilled by the model within 10 per cent. Our model is in agreement with the conclusion that the most sensitivity to mass breaking effects might be expected from the form factors  $h_{A_2}(\omega)$  and  $h_V(\omega)$ . The form factor  $h_{A_1}(1)$  is close to one, as implied by Luke's theorem [39].

Concluding this section we now briefly summarize our main results for heavy to light transitions.

Note that the subject of  $\eta$ ,  $\eta'$  mixing is not touched. Such mixing may be generated in a natural way though instanton effects [29], or two gluon exchanges. Since none of the above forces have been considered here, decays into  $\eta$  or  $\eta'$  are excluded in the calculation. At the present stage it would require additional assumptions and the introduction of mixing parameters, which we like to exclude here.

Concerning pure leptonic decays of light mesons, the description fails badly in a nonrelativistic treatment. In particlar, the value of the pion decay constant  $f_\pi$  turns out to be much too large. Even with the inclusion of the above mentioned

relativistic effects in the current, the framework does not lead to a satisfactory result. Still, it is possible to reproduce the pion mass in the framework given here, see Fig. 1. Obviously a consistent description of mass spectra and decay observables of light mesons can not be achieved in a nonrelativistic framework, compare [28] who introduced ‘mock’ mesons with mass  $\mu = m_q + m_{\bar{q}}$  to describe decay data. Some progress has been achieved using the Bethe Salpeter equation for light  $q\bar{q}$  systems, and spectra as well as decays of light mesons can be described [20].

With this in mind, one has to be careful in interpreting decays involving (very) light mesons in the final state.

The form factors, viz.  $B(D^{(*)}) \rightarrow K, K^*, \pi, \rho, \omega$  and  $D_s \rightarrow K, K^*, \phi$  differ from the pole dominance hypothesis at  $q^2 = q_{max}^2$ , viz. small three momentum transfer [40]. However, they lead to similar values as in the relativistic harmonic oscillator model at  $q^2 = 0$  [21].

Where experimental data is given, we compare our results of the total branching ratios of  $D$ -meson decays and find a rather good agreement. Results are shown in Table 5.

## 4 Nonleptonic decays

Nonleptonic weak decays provide additional phenomena that are connected to strong interaction. Examples are hard gluon exchanges, quark rearrangement, annihilation and long range effects. Thus, extraction of fundamental physical constants such as the Cabibbo-Kobayashi-Maskawa matrix elements is more difficult than in the semileptonic case.

Following [32] we introduce the effective Lagrangian for  $\Delta B = 1$  transitions including QCD-effects but neglecting pinguin contributions [41],

$$\mathcal{L}_{eff} = -\frac{G_F}{\sqrt{2}} \sum_{\alpha' \alpha \beta} V_{\alpha' b} V_{\alpha \beta}^* (C_1(m) h_{\mu, \alpha \beta} h_{\alpha' b}^\mu + C_2(m) h_{\mu, \alpha' \beta} h_{\alpha b}^\mu) \quad (29)$$

with  $\alpha, \alpha' \in \{u, c\}$ ,  $\beta \in \{d, s\}$ , and the Wilson coefficients  $C_1(m)$ ,  $C_2(m)$  depending on the scale  $m$ . For the scale  $m_c \simeq 1.5$  GeV one expects  $C_1(m_c) = 1.27$  and  $C_2(m_c) = -0.53$ , and for  $m_b \simeq 5$  GeV the resulting values are  $C_1(m_b) = 1.12$  and  $C_2(m_b) = -0.26$  [36]. Note that if no additional gluon exchanges are assumed in the operator, the Lagrangian (29) reduces to the nonleptonic weak Langrangian in current current approximation since then  $C_1(m) = 1$  and  $C_2(m) = 0$ .

The Lagrangian (29) is evaluated between the meson amplitudes given in (15). If final state interaction (*fsi*) is neglected, the transition amplitude factorizes. Due to Fierz rearrangement two generic types of contributions are possible. The generic form of class I is given by (30) those of class II by (31), class III are mixed forms of both e.g.  $B^- \rightarrow D^0 \pi^-$ .

$$\langle \pi^+ D^- | h_{\mu, ud} h_{cb}^\mu | B^0 \rangle \rightarrow a_1 \langle \pi^+ | h_{\mu, ud} | 0 \rangle \langle D^- | h_{cb}^\mu | B^0 \rangle \quad (30)$$

$$\left\langle \pi^0 | D^0 | h_{\mu,ud} h_{cb}^\mu | B^0 \right\rangle \rightarrow a_2 \left\langle D^0 | h_{\mu,cd} | 0 \right\rangle \left\langle \pi^0 | h_{ub}^\mu | B^0 \right\rangle \quad (31)$$

where we have introduced  $a_1$  and  $a_2$ , to connect our results with the model of BSW [21]. In the above case  $a_1 = 1$  and from Fierz rearrangement  $a_2 = 1/3$ . If gluonic contributions are taken into account,  $a_1 = C_1(m) + \xi C_2(m)$  and  $a_2 = C_2(m) + \xi C_1(m)$ , with  $\xi = 1/3$ .

In fact BSW have introduced  $a_1$  and  $a_2$  on the level of the effective Lagrangian and assume  $h_{\alpha\beta}$  to depend only on asymptotic hadronic (interpolating) fields. This introduces problems in interpreting  $a_1$  and  $a_2$  in terms of the Wilson coefficients and therefore  $a_1$  and  $a_2$  are usually treated as free parameters, see discussion in [21] and references therein. Since we have introduced wave functions for the mesons, which connect quark degrees of freedom with asymptotic degrees of freedom these parameters have a different interpretation as in BSW. However, the general problems discussed in [21] remain the same, and  $a_1$  and  $a_2$  can be treated as free parameters in the wave function approach also. Since the same approximations are done when calculating matrix elements, our values of  $a_1$  and  $a_2$  are compatible with those given by BSW.

Evaluation of the r.h.s. of (30) and (31) using quark model wave functions leads to some uncertainty connected to light mesons. As already mentioned in the previous section light mesons are not well described. Part of the uncertainty related e.g. to the transition matrix element  $\langle X | h_\mu | 0 \rangle$  can be removed by using empirical decay constants instead of calculated ones. From leptonic weak decays these are available only for  $\pi$  and  $K$  decays. For the  $D$ -meson an upper limit exists,  $f_{D^+} < 310\text{MeV}$ . For  $f_{D_s}$  we have chosen  $f_{D_s} = 300\text{MeV}$ , which is a good fit of our model to the branching ratios measured (see Table 9), and is close to values found by Rosner [37] and an ARGUS analysis using different type of model analyses [38]. For  $f_\rho$  we have used  $f_\rho = 205\text{MeV}$ , which has been suggested by [43]. Other decay constants are taken from [21] and listed in Table 6.

The problem of factorization usually discussed in this context is not further elaborated here, see [21, 22, 42]. Through the use of wave functions many important questions related to the factorization hypothesis have to be rephrased (e.g. color octet excitations vs. model space etc.). Model independent tests of factorization have been suggested by Kamal, Xu and Czarnecki, who found that even in cases of heavy to light-light (except  $D^0 \rightarrow K^- a_1^+$ ), factorization seems reasonable, provided the final state interaction is properly taken into account [23].

We consider the following combinations of decays  $0^- \rightarrow 0^-(0^-)$ ,  $0^- \rightarrow 0^-(1^-)$ ,  $0^- \rightarrow 0^-(1^+)$ ,  $0^- \rightarrow 1^-(0^-)$ ,  $0^- \rightarrow 1^-(1^-)$ , and  $0^- \rightarrow 1^-(1^+)$ . The quantum numbers of the meson due to vacuum to meson transition is given in parenthesis. Experimental data are taken from the compilation of the Particle Data Group [35]. However, were new data exist, we have updated the average values using the latest results of CLEO [34] and ARGUS [38, 31] collaborations.

In each of the following tables 9-12 we have given the type of decay, our calculated decay rate excluding CKM matrix elements and decay constants, our

decay rate in terms of  $a_1$  and/or  $a_2$ , which may be compared with the respective rates of BSW [21, 43], and in the last column the experimental value where available. The decay parameters used are quoted in Table 6. The Cabibbo Kobayashi Maskawa matrix elements used are given in Table 7.

From  $\overline{B}^0 \rightarrow D^+ \pi^-$ ,  $\overline{B}^0 \rightarrow D^+ \rho^-$ ,  $\overline{B}^0 \rightarrow D^{*+} \pi^-$ , and  $\overline{B}^0 \rightarrow D^{*+} \rho^-$  decays we find a best fit to the data for  $a_1 = (0.96 \pm 0.05)(0.036/V_{cb})(1.32ps/\tau_B)^{1/2}$ . Inclusion of all decays in  $\chi^2$  fitting leads to essentially no change on  $a_1$ .

For  $a_2$  we find  $|a_2| = 0.31 \pm 0.03$  as a best fit to the data. Including recent CLEO data, we find the relative sign between  $a_1$  and  $a_2$  positive in the following sense. The total  $\chi^2$  from the decays  $B^- \rightarrow D^0 \pi^-$ ,  $B^- \rightarrow D^{*0} \pi^-$ ,  $B^- \rightarrow D^0 \rho^-$ , and  $B^- \rightarrow D^{*0} \rho^-$  is  $\chi^2_+ \simeq 2.6$  for the plus sign and for the minus sign  $\chi^2_- \simeq 25$ . Details are given in Table 12.

Some experimental uncertainties may be eliminated using ratios of branching ratios, and with the assumption  $f_{D_s} = f_{D_s^*}$  less ambiguous comparisons can be made. In table 8 we have compared our results to recent ARGUS data [38].

## 5 Summary and Conclusion

We have calculated  $\overline{q}q$  spectra within a nonrelativistic framework with forces expanded up to order  $(p/m)^2$ . Not all terms in the Hamiltonian are equally important. Those of minor importance are left out for convenience. We find parameter values in a reasonable range and close to those of the Cornell potential (where comparison is possible). Spectra for all mesons are reproduced reasonably well. We have, however, excluded the question of  $\eta$ ,  $\eta'$  mixing, which is not expected to influence the conclusion reached in this section.

We have included the full Dirac quark spinor to define the appropriate current operators for the meson Fock space. Compared to the nonrelativistic approach we found important effects on decay constants and form factors.

Since we use physical masses, the Isgur Wise function cannot be calculated. However, we find that at  $\omega = 1$  the normalization of the form factors is within 10% of the heavy quark limit expectations.

Assuming the lifetime of  $B$ -meson  $\tau_B = 1.32ps$ , which is longer than given in the last edition of particle data tables [35], but still shorter than most recent values, we find  $V_{cb} = 0.036 \pm 0.003$ .

Concerning nonleptonic decays, the best values for  $a_1$  and  $a_2$  suggest that hard gluon exchanges may be neglected, viz.  $C_2(m_b) \simeq 0$ . A similar conclusion is possible for charmonium and bottomonium within the framework of the quark model presented here, see discussion in [13]. Gluonic effects have been found to accommodate experimental data only in a pure nonrelativistic approach of lowest order. However, if relativity is treated more appropriately, inclusion of gluonic effects destroy the rather good agreement with quarkonium data [13].

Other suggestions are also possible. For example, if the color factor  $\xi$  introduced after (31) were changed to  $\xi \simeq 1/2$ , then  $a_1 = 0.99$  and  $a_2 = 0.30$  at the  $B$  meson mass scale. These numbers are also in reasonable agreement with the value extracted here. This might imply that ‘color octett’ contributions are not negligible.

However, at the present stage of analysis we would like to emphasize that the above possibilities are mere speculations, which however call for further investigation. It seems that the situation has never been as puzzling as at the moment. Since relativistic effects seem to play a nonnegligible role, some progress can be expected from recent developments using Bethe-Salpeter equation taking covariance seriously.

We have not considered nonleptonic  $D$  decays in the paper. No reasonable  $\chi^2$  could be found for a fit of  $a_1$  and  $a_2$ . It is well known that these decays are more biased by  $fsi$  and relativistic effects, which we did not take into account. Also the model (being generically nonrelativistic) should be less reliable in these cases.

## References

- [1] A. De Rújula, H. Georgi, S.L. Glashow: Phys. Rev. D 12 (1975) 147
- [2] E. Eichten et al.: Phys. Rev. D 17 (1978) 3090; D 21 (1980) 203
- [3] C. Quigg, J.L. Rosner: Phys. Lett. 21B (1977) 252; W. Kwong, J.L. Rosner, C. Quigg: Ann. Rev. Nucl. Part. Sci. 37 (1987) 325
- [4] W. Celmaster, H. Georgi, M. Machazek: Phys. Rev. D17 (1978) 879
- [5] G. Bhanot, S. Rudaz: Phys. Lett. 78B (1978) 119
- [6] J. Richardson: Phys. Lett. 82B (1979) 272
- [7] G. Fogleman, D.B. Lichtenberg, J.G. Wills: Lett. Nuovo Cim. 26 (1979) 369
- [8] W. Buchmüller, S.-H. Tye: Phys. Rev. D 24 (1981) 132
- [9] A. Martin: Phys. Lett. 93B (1980) 338; 100B (1981) 511
- [10] X.T. Song, H. Lin: Z. Phys. C - Particles and Fields 34 (1987) 223
- [11] D.B. Lichtenberg et al.: Z. Phys. C - Particles and Fields 41 (1989) 615
- [12] D.B. Lichtenberg, R. Roncaglia, L.G. Wills: Z. Phys. C - Particles and Fields 46 (1990) 75
- [13] M. Beyer, U. Bohn, M.G. Huber, B.C. Metsch, J. Resag, Z. Phys. C - Particles and Fields 55 (1992) 307
- [14] D.B. Lichtenberg: Int. J. Mod. Phys. A2 (1987) 1669
- [15] W. Lucha, F.F. Schöberl, D. Gromes: Phys. Rep. 200 (1991) 127
- [16] J. Resag, diploma thesis Bonn 1992, unpublished
- [17] J.F. Lagaë: Phys. Rev. D45 (1992) 305, 317
- [18] H. Hersbach: Phys. Rev. A46 (1992) 3657, D47 (1993) 3027, Utrecht THU-93/13 (1993)
- [19] P.C. Tiemeijer, J.A. Tjon: Phys. Lett. B 277 (1992), Utrecht THU-92/31, THU-93/12
- [20] J. Resag, C.R. Münz, B.C. Metsch, H.R. Petry: BONN TK-93-13 (nucl-th/9307026); C.R. Münz, J. Resag, B.C. Metsch, H.R. Petry: BONN TK-93-14 (nucl-th/9307027)

- [21] M. Bauer, B.Stech, and M. Wirbel, Z. Phys. C - Particles and Fields 34 (1987) 103; M. Wirbel, Prog. in Nucl. Part. Phys. 22 (1988) 33
- [22] J.D. Bjorken, Nucl. Phys. B (Proc. Suppl.) 11 (1989) 325
- [23] A.N. Kamal, Q.P. Xu, and A. Czarnecki, preprint Alberta Thy-3-93
- [24] M. Neubert, SLAC-PUB-6263, June 1993
- [25] N. Isgur, M. B. Wise, Phys. Lett. B 232, 113 (1989); B 237, 527 (1990)
- [26] R. McClary, N. Byers: Phys. Rev. D28 (1983) 1692
- [27] U. Bohn, BONN TK-89-08 (diploma thesis, unpublished)
- [28] S. Godfrey, N. Isgur: Phys. Rev. D 32 (1985) 189
- [29] G. 't Hooft: Phys. Rev. D 14 (1976) 3432
- [30] R. Van Royen, V.F. Weisskopf: Nuovo Cimento 50, 2A (1967) 517
- [31] H. Albrecht et al., ARGUS Coll: Z. Phys. C - Particles and Fields 57 (1993) 533
- [32] J.G. Körner, G.A. Schuler: Z. Phys.- Particles and Fields C 38, (1988) 511[E: C 41, (1989) 690]; C 46, (1990) 93
- [33] D.G. Cassel, CLEO Coll.: (private communication)
- [34] S. Sanghera et al., CLEO Coll.: Phys. Rev. D 47, (1993) 791 - 798
- [35] K. Hikasa et al., Particle Data Group: Phys. Rev. D 45 II (1992)
- [36] G. Altarelli, L. Maiani: Phys. Lett. B52 (1974) 351; M.K. Gaillard, B.W. Lee: Phys. Rev. Lett. 33 (1974) 108
- [37] J.L. Rosner: Phys. Rev. D42 (1990) 3732
- [38] H. Albrecht et al., ARGUS Coll.: Z. Phys. C - Particles and Fields 54 (1992) 1
- [39] M.E. Luke: Phys. Lett. B 252 (1990) 447
- [40] S. Resag: diploma thesis (unpublished) BONN TK-93-17
- [41] M.A. Shifman, A.I. Weinstein, V.I. Zakharov: Nucl. Phys. B147 (1979) 382, 448
- [42] A.J. Buras, J.-M. Gérard, R. Rückl: Nucl. Phys. B268 (1986) 16
- [43] M. Neubert, V. Rieckert, B.Stech, Q.P. Xu: *Heavy Flavours*, A.J. Buras and M. Lindner eds. (Singapore 1992) p. 286.

Table 1: Parameter values of the Hamiltonian. \*For mesons other than  $B$ -, and  $D_{(s)}^{(*)}$ -mesons we have used  $r_0 = 0.30\text{fm}$

$m_n$ [GeV]	0.411
$m_s$ [GeV]	0.594
$m_c$ [GeV]	1.806
$m_b$ [GeV]	5.183
$a$ [GeV]	-0.668
$b$ [GeV/fm]	0.792
$\alpha_s$	0.41
$r_0$ [fm]*	0.24

Table 2: Pole masses (in GeV) for  $B \rightarrow D$  and  $B \rightarrow D^*$  form factors

$F_0$	$F_1, V$	$A_1, A_2$	$A_0$
6.80	6.34	6.37	6.3

Table 3: Branching ratios for B decays. We use  $\tau_B = 1.32\text{ps}$ , a) recent CLEO, b) recent ARGUS data

decay	$Br_{QM}[\%]$	$Br_{exp}[\%]$
$\bar{B}^0 \rightarrow D^{*+} \ell^- \bar{\nu}_\ell$	4.5	$4.9 \pm 0.8$
		$4.50 \pm 0.44 \pm 0.44^a$
$\bar{B}^0 \rightarrow D^+ \ell^- \bar{\nu}_\ell$	1.8	$5.2 \pm 0.5 \pm 0.6^b$
		$1.6 \pm 0.7$

Table 4: Parameters for a fit to the dominant formfactors

	$h_+$	$h_V$	$h_{A_1}$	$h_{A_3}$
$h(1)$	0.993	0.896	0.977	0.945
$\beta$	0.47	0.58	0.58	0.58

Table 5: Branching ratios for D decays. We use  $\tau_{D^0} = 0.42\text{ps}$ ,  $\tau_{D^+} = 1.066\text{ps}$ ,  $\tau_{D_s} = 0.45\text{ps}$

decay	$Br_{QM}[\%]$	$Br_{exp}[\%]$
$D^+ \rightarrow \bar{K}^0 e^+ \bar{\nu}_e$	7.64	$5.5 \pm 1.2$
$D^+ \rightarrow \bar{K}^0 \mu^+ \bar{\nu}_\mu$	7.64	$7.0 \pm 3.0$
$D^+ \rightarrow \bar{K}^{*0} e^+ \bar{\nu}_e$	6.43	$4.1 \pm 0.6$
$D^0 \rightarrow K^- e^+ \bar{\nu}_e$	3.01	$3.31 \pm 0.29$
$D^0 \rightarrow K^- \mu^+ \bar{\nu}_\mu$	3.01	$2.9 \pm 0.5$
$D^0 \rightarrow K^{*-} e^+ \bar{\nu}_e$	2.53	$1.7 \pm 0.6$
$D^s \rightarrow \phi \ell^+ \bar{\nu}_\ell$	2.41	$1.4 \pm 0.5$

Table 6: Leptonic decay constants used in the calculation

weak current	meson type	$f$ [MeV]	weak current	meson type	$f$ [MeV]
$\bar{u}d$	$\pi^-$	132	$\bar{u}d$	$\rho^-$	205
$\bar{d}d$	$\pi^0$	93	$\bar{d}d$	$\rho^0$	145
$\bar{u}s$	$K^-$	162	$\bar{u}d$	$K^{*-}$	220
$\bar{d}s$	$\bar{K}^0$	162	$\bar{u}d$	$\bar{K}^{*0}$	220
$\bar{d}c$	$D^+$	220	$\bar{d}c$	$D^{*+}$	220
$\bar{u}c$	$D^0$	220	$\bar{u}c$	$D^{*0}$	220
$\bar{s}c$	$D_s^+$	300	$\bar{s}c$	$D_s^{*+}$	300
			$\bar{d}d$	$\omega$	145
			$\bar{c}c$	$J/\Psi$	382
			$\bar{u}d$	$a_1^-$	220

Table 7: Parameters used in the calculation of non-leptonic decays

$V_{ud}$	$V_{us}$	$V_{ub}$	$V_{cd}$	$V_{cs}$	$V_{cb}$
0.9753	0.221	-	0.221	0.9743	0.036

Table 8: Comparison of ratios of branching ratios, upper part ARGUS data [38]

$\frac{Br(B^- \rightarrow D_s^{*-} D^0)}{Br(B^- \rightarrow D_s^- D^0)}$	$\frac{Br(B^- \rightarrow D_s^{*-} D^{*0})}{Br(B^- \rightarrow D_s^- D^{*0})}$	$\frac{Br(B^0 \rightarrow D_s^{*-} D^+)}{Br(B^0 \rightarrow D_s^- D^+)}$	$\frac{Br(B^0 \rightarrow D_s^{*-} D^{*+})}{Br(B^0 \rightarrow D_s^- D^{*+})}$
$0.67 \pm 0.65$	$2.4 \pm 2.1$	$1.6 \pm 1.5$	$1.9 \pm 1.6$
0.63	3.3	0.63	3.3

Table 9: Class I  $B$  decay and branching ratios due to  $\bar{c}b$  current. Model calculation with  $a_1 = 0.96(0.036/V_{cb})(1.32ps/\tau_B)^{1/2}$ , for normalization of  $B \rightarrow D^{(*)}D_s^{(*)}$  decays we have used  $Br(D_s^+ \rightarrow \phi\pi^+) = 2.7\%$  as suggested by ARGUS.

decay mode	quark model		experiment Br[%]
	$\Gamma[10^8 s^{-1}]$	Br[%]	
$\overline{B}^0 \rightarrow D^+ \pi^-$	$1.233V_{cb}^2 V_{ud}^2 f_\pi^2 a_1^2 \rightarrow 0.350 a_1^2$	0.322	$0.29 \pm 0.05$
$\overline{B}^0 \rightarrow D^+ \rho^-$	$1.162V_{cb}^2 V_{ud}^2 f_\rho^2 a_1^2 \rightarrow 0.795 a_1^2$	0.732	$0.73 \pm 0.21$
$\overline{B}^0 \rightarrow D^+ a_1^-$	$1.038V_{cb}^2 V_{ud}^2 f_{a_1}^2 a_1^2 \rightarrow 0.818 a_1^2$	0.753	$0.60 \pm 0.33$
$\overline{B}^0 \rightarrow D^{*+} \pi^-$	$0.953V_{cb}^2 V_{ud}^2 f_\pi^2 a_1^2 \rightarrow 0.270 a_1^2$	0.249	$0.30 \pm 0.05$
$\overline{B}^0 \rightarrow D^{*+} \rho^-$	$1.093V_{cb}^2 V_{ud}^2 f_\rho^2 a_1^2 \rightarrow 0.747 a_1^2$	0.689	$0.74 \pm 0.17$
$\overline{B}^0 \rightarrow D^{*+} a_1^-$	$1.304V_{cb}^2 V_{ud}^2 f_{a_1}^2 a_1^2 \rightarrow 1.027 a_1^2$	0.947	$1.80 \pm 0.85$
$\overline{B}^0 \rightarrow D^+ D_s^-$	$1.072V_{cb}^2 V_{cs}^2 f_{D_s}^2 a_1^2 \rightarrow 1.567 a_1^2$	1.444	$0.84 \pm 0.51$
$\overline{B}^0 \rightarrow D^+ D_s^{*-}$	$0.674V_{cb}^2 V_{cs}^2 f_{D_s^*}^2 a_1^2 \rightarrow 0.985 a_1^2$	0.908	$2.7 \pm 1.9$
$\overline{B}^0 \rightarrow D^{*+} D_s^-$	$0.524V_{cb}^2 V_{cs}^2 f_{D_s}^2 a_1^2 \rightarrow 0.765 a_1^2$	0.705	$1.42 \pm 0.75$
$\overline{B}^0 \rightarrow D^{*+} D_s^{*-}$	$1.721V_{cb}^2 V_{cs}^2 f_{D_s^*}^2 a_1^2 \rightarrow 2.515 a_1^2$	2.318	$2.6 \pm 1.5$
$\overline{B}^0 \rightarrow D^+ K^-$	$1.227V_{cb}^2 V_{us}^2 f_K^2 a_1^2 \rightarrow 0.027 a_1^2$	0.025	—
$\overline{B}^0 \rightarrow D^+ K^{*-}$	$1.137V_{cb}^2 V_{us}^2 f_{K^*}^2 a_1^2 \rightarrow 0.046 a_1^2$	0.042	—
$\overline{B}^0 \rightarrow D^{*+} K^-$	$0.928V_{cb}^2 V_{us}^2 f_K^2 a_1^2 \rightarrow 0.020 a_1^2$	0.019	—
$\overline{B}^0 \rightarrow D^{*+} K^{*-}$	$1.138V_{cb}^2 V_{us}^2 f_{K^*}^2 a_1^2 \rightarrow 0.046 a_1^2$	0.042	—
$\overline{B}^0 \rightarrow D^+ D^-$	$1.093V_{cb}^2 V_{cd}^2 f_D^2 a_1^2 \rightarrow 0.044 a_1^2$	0.041	—
$\overline{B}^0 \rightarrow D^+ D_s^{*-}$	$0.726V_{cb}^2 V_{cd}^2 f_{D_s^*}^2 a_1^2 \rightarrow 0.029 a_1^2$	0.027	—
$\overline{B}^0 \rightarrow D^{*+} D^-$	$0.565V_{cb}^2 V_{cd}^2 f_D^2 a_1^2 \rightarrow 0.023 a_1^2$	0.021	—
$\overline{B}^0 \rightarrow D^{*+} D_s^{*-}$	$1.682V_{cb}^2 V_{cd}^2 f_{D_s^*}^2 a_1^2 \rightarrow 0.068 a_1^2$	0.063	—
$B^- \rightarrow D^0 a_1^-$	$1.038V_{cb}^2 V_{ud}^2 f_{a_1}^2 a_1^2 \rightarrow 0.818 a_1^2$	0.753	$0.45 \pm 0.36$
$B^- \rightarrow D^{*0} a_1^-$	$1.304V_{cb}^2 V_{ud}^2 f_{a_1}^2 a_1^2 \rightarrow 1.027 a_1^2$	0.947	—
$B^- \rightarrow D^0 D_s^-$	$1.072V_{cb}^2 V_{cs}^2 f_{D_s}^2 a_1^2 \rightarrow 1.567 a_1^2$	1.444	$2.0 \pm 0.8$
$\overline{B}^- \rightarrow D^0 D_s^{*-}$	$0.674V_{cb}^2 V_{cs}^2 f_{D_s^*}^2 a_1^2 \rightarrow 0.985 a_1^2$	0.908	$1.6 \pm 1.2$
$\overline{B}^- \rightarrow D^{*0} D_s^-$	$0.524V_{cb}^2 V_{cs}^2 f_{D_s}^2 a_1^2 \rightarrow 0.765 a_1^2$	0.705	$1.3 \pm 0.9$
$\overline{B}^- \rightarrow D^{*0} D_s^{*-}$	$1.72V_{cb}^2 V_{cs}^2 f_{D_s^*}^2 a_1^2 \rightarrow 2.514 a_1^2$	2.317	$3.1 \pm 1.7$
$\overline{B}^- \rightarrow D^0 D^-$	$1.093V_{cb}^2 V_{cd}^2 f_D^2 a_1^2 \rightarrow 0.044 a_1^2$	0.041	—
$\overline{B}^- \rightarrow D^0 D^{*-}$	$0.726V_{cb}^2 V_{cd}^2 f_{D^*}^2 a_1^2 \rightarrow 0.029 a_1^2$	0.027	—
$\overline{B}^- \rightarrow D^{*0} D^-$	$0.565V_{cb}^2 V_{cd}^2 f_D^2 a_1^2 \rightarrow 0.013 a_1^2$	0.021	—

Table 10: Class I  $B$  decay and branching ratios due to  $\bar{u}b$  current,  $\tilde{a}_1 = a_1(V_{bu}/V_{bc})$

decay mode	quark model			experiment
	$\Gamma[10^8 s^{-1}]$	Br[%]	Br[%]	
$\bar{B}^0 \rightarrow \pi^+ \pi^-$	$0.170 V_{ub}^2 V_{ud}^2 f_\pi^2 a_1^2 \rightarrow 0.048 \tilde{a}_1^2$	0.044	$(V_{bu}/V_{bc})^2$	< 0.009
$\bar{B}^0 \rightarrow \pi^+ \rho^-$	$0.176 V_{ub}^2 V_{ud}^2 f_\rho^2 a_1^2 \rightarrow 0.120 \tilde{a}_1^2$	0.111	$(V_{bu}/V_{bc})^2$	—
$\bar{B}^0 \rightarrow \pi^+ a_1^-$	$0.185 V_{ub}^2 V_{ud}^2 f_{a_1}^2 a_1^2 \rightarrow 0.146 \tilde{a}_1^2$	0.136	$(V_{ub}/V_{bc})^2$	< 0.057

Table 11: Class II  $B$  decay and branching ratios,  $|a_2| = 0.31$

decay mode	quark model			experiment
	$\Gamma[10^8 s^{-1}]$	Br[%]	Br[%]	
$\bar{B}^0 \rightarrow \pi^0 D^0$	$0.111 V_{cb}^2 V_{ud}^2 f_\pi^2 a_2^2 \rightarrow 0.087 a_2^2$	0.008	—	—
$\bar{B}^0 \rightarrow \pi^0 D^{*0}$	$0.104 V_{ub}^2 V_{ud}^2 f_{D^*}^2 a_2^2 \rightarrow 0.082 a_2^2$	0.008	—	—
$\bar{B}^0 \rightarrow K^0 J/\Psi$	$0.320 V_{cb}^2 V_{cs}^2 f_{J/\Psi}^2 a_2^2 \rightarrow 0.759 a_2^2$	0.073	$0.077 \pm 0.026$	—
$\bar{B}^0 \rightarrow K^{*0} J/\Psi$	$0.732 V_{cb}^2 V_{cs}^2 f_{J/\Psi}^2 a_2^2 \rightarrow 1.735 a_2^2$	0.167	$0.14 \pm 0.03$	—
$\bar{B}^0 \rightarrow K^{*0} D^{*0}$	$0.524 V_{cb}^2 V_{us}^2 f_{D^*}^2 a_2^2 \rightarrow 0.021 a_2^2$	0.002	—	—
$\bar{B}^0 \rightarrow \pi^0 J/\Psi$	$0.231 V_{cb}^2 V_{cd}^2 f_{J/\Psi}^2 a_2^2 \rightarrow 0.028 a_2^2$	0.003	—	—
$B^- \rightarrow K^- J/\Psi$	$0.320 V_{cb}^2 V_{cs}^2 f_{J/\Psi}^2 a_2^2 \rightarrow 0.759 a_2^2$	0.073	$0.090 \pm 0.014$	—
$B^- \rightarrow K^{*-} J/\Psi$	$0.732 V_{cb}^2 V_{cs}^2 f_{J/\Psi}^2 a_2^2 \rightarrow 1.735 a_2^2$	0.167	$0.16 \pm 0.05$	—
$B^- \rightarrow \pi^- J/\Psi$	$0.463 V_{cb}^2 V_{cd}^2 f_{J/\Psi}^2 a_2^2 \rightarrow 0.056 a_2^2$	0.005	—	—

Table 12: Class III (mixed)  $B$  branching ratios

decay mode	quark model Br[%]			experiment
	$a_2 > 0$	$a_2 < 0$	Br[%]	
$B^- \rightarrow D^0 \pi^-$	$0.344 (a_1 + 0.52a_2)^2$	0.433	0.220	$0.38 \pm 0.05$
$B^- \rightarrow D^{*0} \pi^-$	$0.266 (a_1 + 0.80a_2)^2$	0.388	0.135	$0.42 \pm 0.10$
$B^- \rightarrow D^0 \rho^-$	$0.795 (a_1 + 0.55a_2)^2$	1.016	0.496	$1.08 \pm 0.27$
$B^- \rightarrow D^{*0} \rho^-$	$1.152 (a_1 + 0.59a_2)^2$	1.507	0.694	$1.11 \pm 0.35$
$B^- \rightarrow D^0 K^-$	$0.027 (a_1 + 0.55a_2)^2$	0.034	0.017	—
$B^- \rightarrow D^0 K^{*-}$	$0.047 (a_1 + 0.46a_2)^2$	0.057	0.031	—

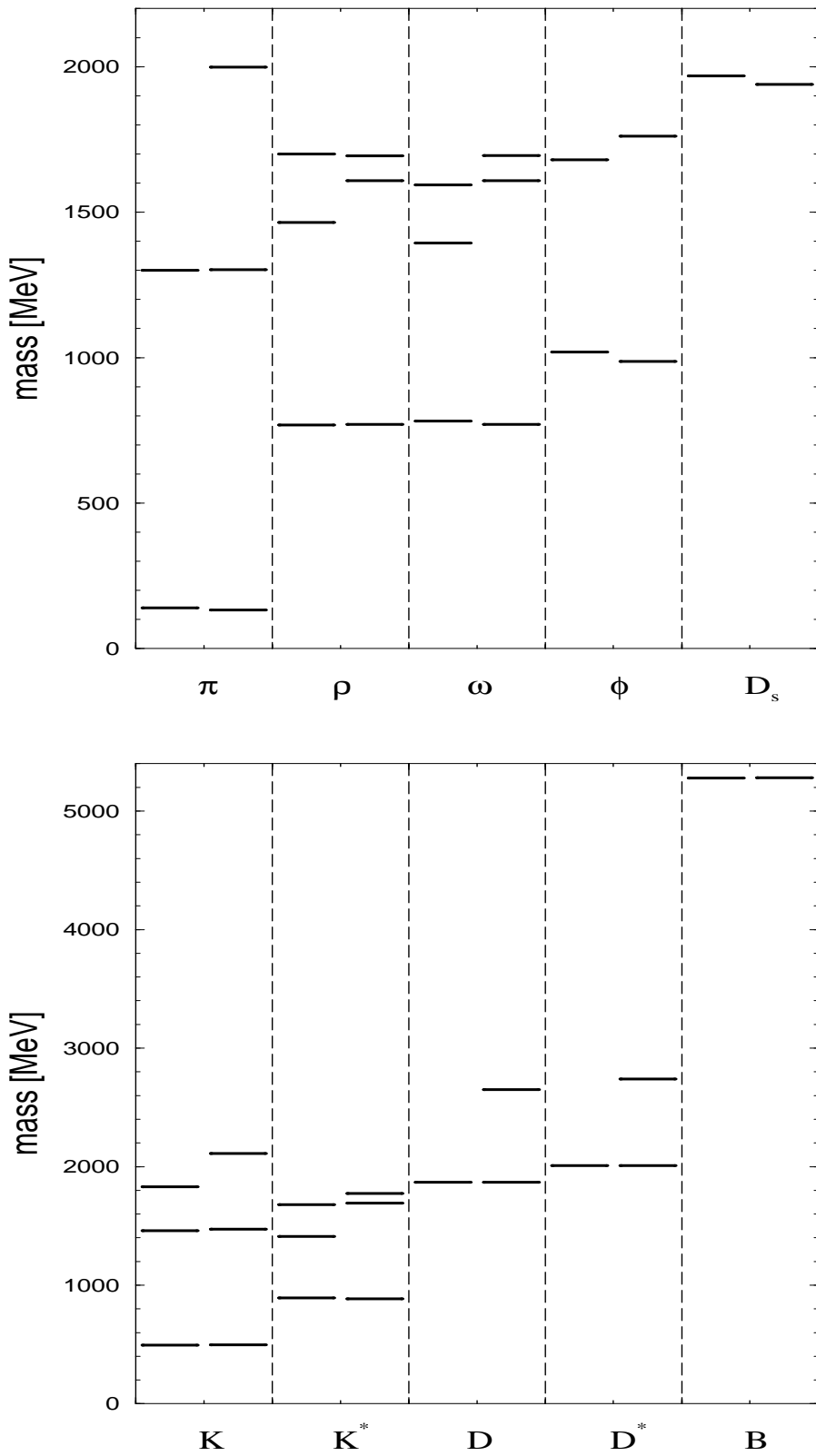


Figure 1: Meson mass spectra of pseudoscalar and vector mesons: The l.h.s. of each column is the experimental data, while the r.h.s. shows the calculated values

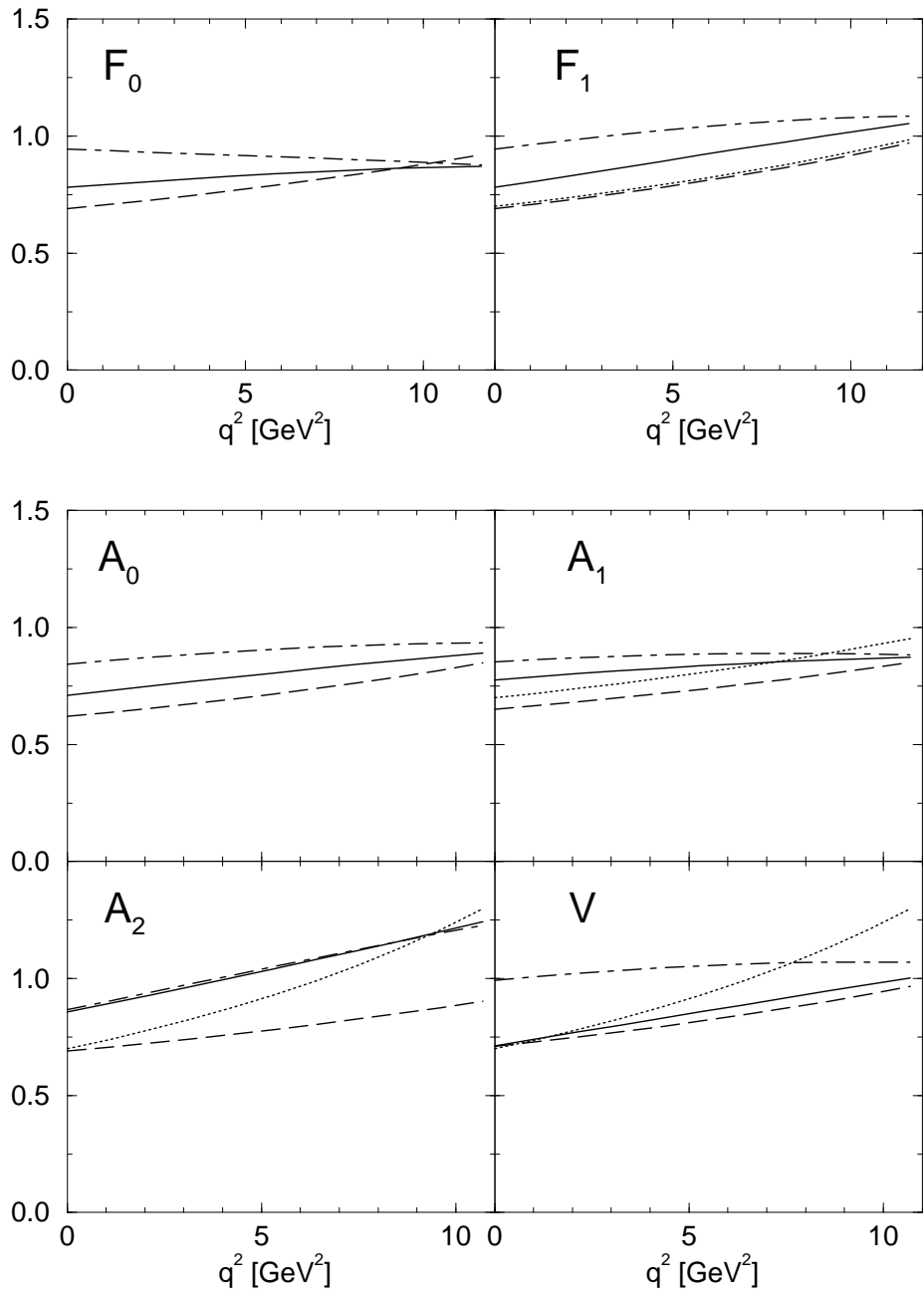


Figure 2: A comparison of form factors for  $B \rightarrow D$  and  $B \rightarrow D^*$  transitions; our full result (solid line), our non relativistic result (dashed-dotted), BSW (dashed), KS (dotted, where given)

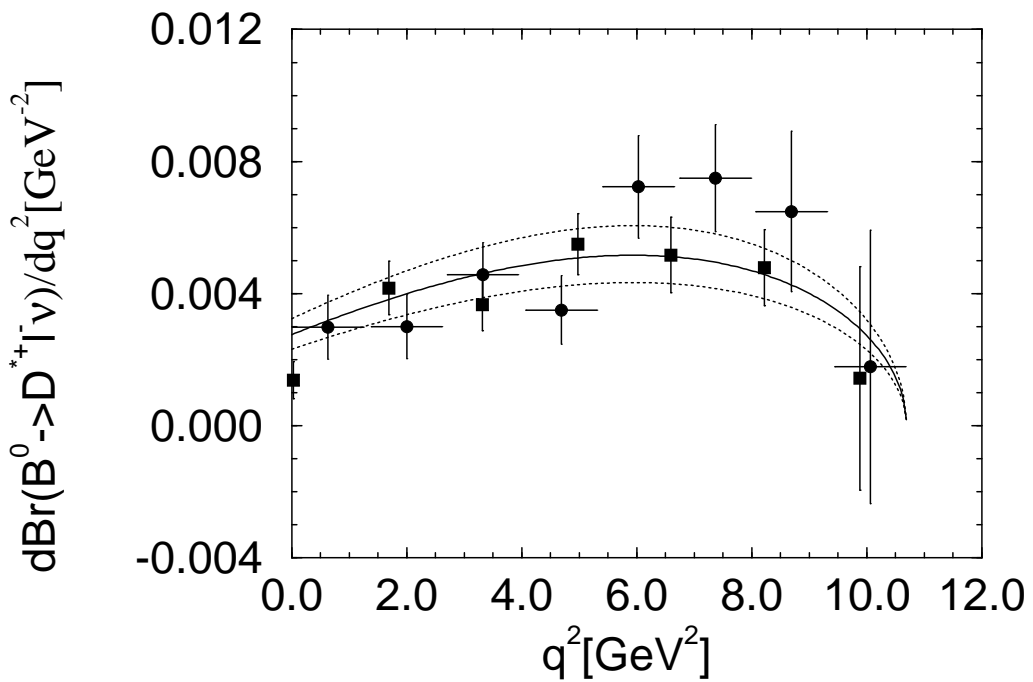


Figure 3:  $q^2$  distribution of  $B^0 \rightarrow D^{*+} \ell^- \bar{\nu}$ . Experiments given by ARGUS (circles) and CLEO (squares). The solid line calculated with  $V_{cb} = 0.036$  and life time  $\tau_B = 1.32ps$ ; the upper and lower dotted lines with  $V_{cb} = 0.036 \pm 0.003$  respectively.

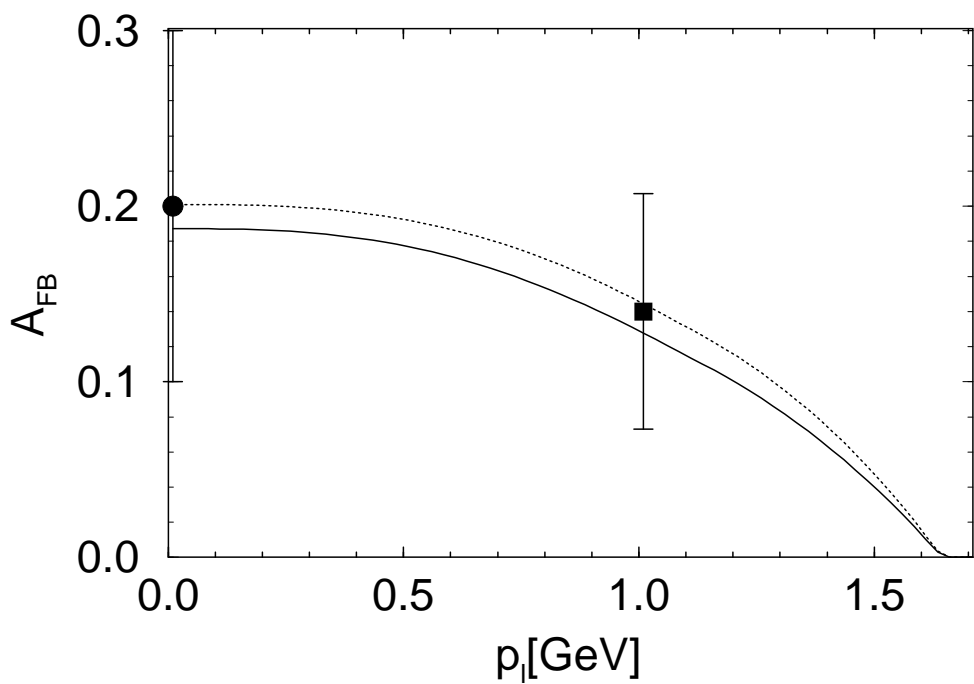


Figure 4: Forward backward asymmetry for  $B^0 \rightarrow D^{*+} \ell^- \bar{\nu}$  as a function of lepton momentum cut experiments ARGUS (circle), CLEO (square)

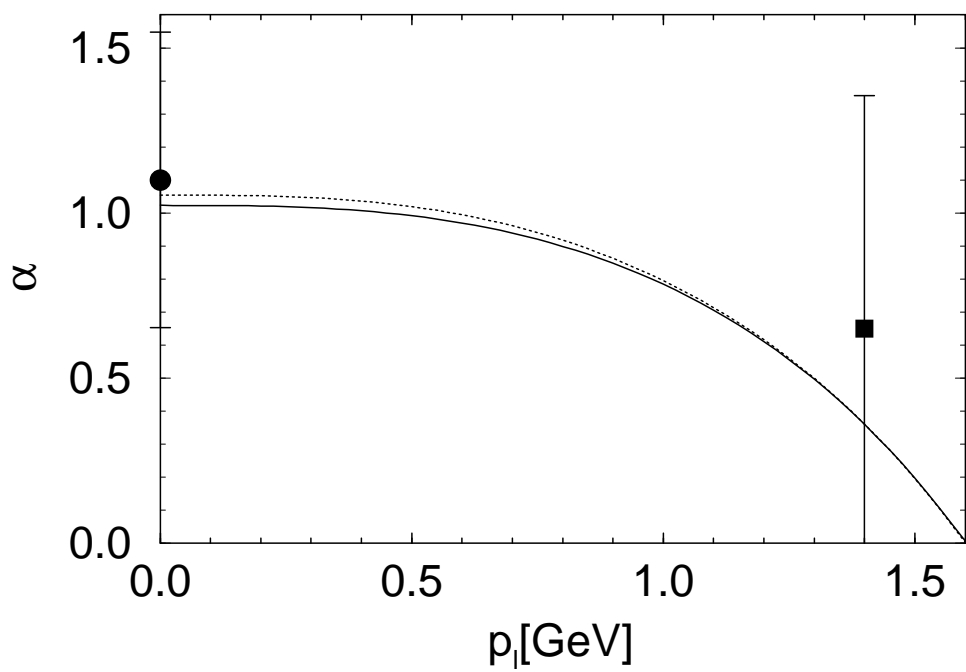


Figure 5: Asymmetry parameter for  $B^0 \rightarrow D^{*+} \ell^- \bar{\nu}$  as function of lepton momentum cut experiments ARGUS (circle), CLEO (square)

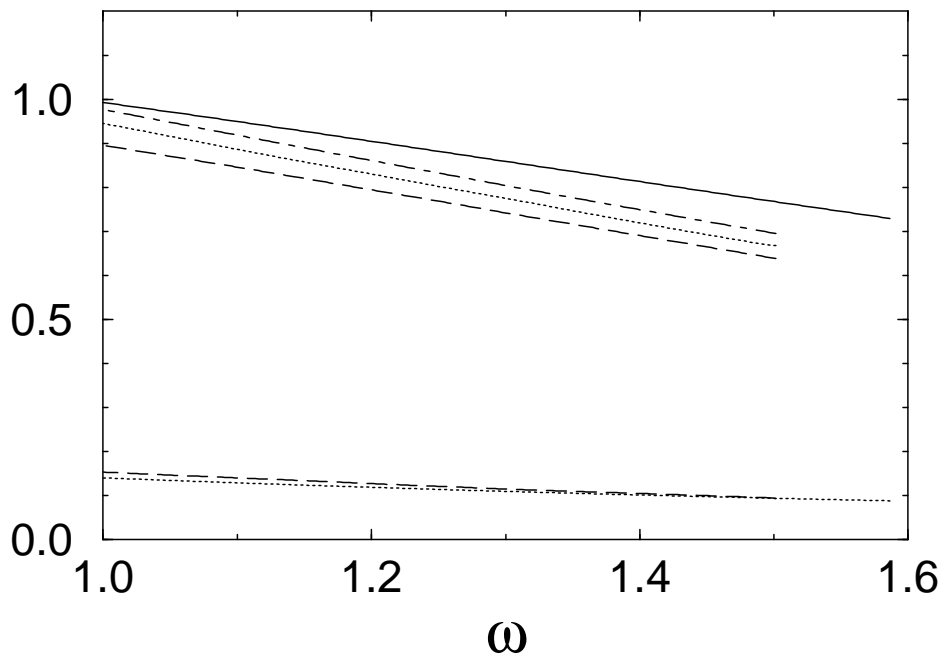


Figure 6: “Heavy quark” form factors for  $B \rightarrow D$  und  $B \rightarrow D^*$  transitions; from top to bottom:  $h_+$ ,  $h_{A_1}$ ,  $h_{A_3}$ ,  $h_V$ ,  $r h_{A_2}$ ,  $h_-$ ,  $r = m_{D^*}/m_B$ .

This figure "fig1-1.png" is available in "png" format from:

<http://arXiv.org/ps/hep-ph/9312298v1>

This figure "fig2-1.png" is available in "png" format from:

<http://arXiv.org/ps/hep-ph/9312298v1>

This figure "fig1-2.png" is available in "png" format from:

<http://arXiv.org/ps/hep-ph/9312298v1>

This figure "fig2-2.png" is available in "png" format from:

<http://arXiv.org/ps/hep-ph/9312298v1>

This figure "fig1-3.png" is available in "png" format from:

<http://arXiv.org/ps/hep-ph/9312298v1>

This figure "fig2-3.png" is available in "png" format from:

<http://arXiv.org/ps/hep-ph/9312298v1>